Adaptive Extended Luenberger Observer in State Feedback Control of Nonlinear Dynamical Systems

Ali Umut Genc
IAV Automative Engineering
UK Branch
Basildon, Essex, UK
umut.genc@ieee.org

Soubhik Auddy
Power Systems Laboratory
University of Western Ontario
London, Ontario, Canada
soubhikauddy@yahoo.com

Deniz Erdogmus
CNEL, ECE Department
University of Florida
Gainesville, Florida, USA
derdogmus@ieee.org

Shyama P. Das
Power Electronics Laboratory
Indian Institute of Technology
Kanpur, India
spdas@iitk.ac.in

Jose C. Principe
CNEL, ECE Department
University of Florida
Gainesville, Florida, USA
princpe@cnel.ufl.edu

Abstract

We have previously proposed an adaptive observer for general nonlinear system state estimation called the adaptive extended Luenberger observer. This observer is similar to the Kalman filter in principle. However, in contrast to the recursive updates of the Kalman filter, this observer uses stochastic gradient updates for the observer gains. In this paper, we demonstrate two successful applications of the proposed adaptive observer scheme in closed-loop state feedback control of realistic nonlinear dynamical systems. Specifically, the problems we consider here are air-to-fuel ratio control in internal combustion engines and direct vector control of an induction machine.

1. Introduction

State estimation for time-varying nonlinear systems has been an important subject in control systems research, since the well-known solution to the optimal state estimation problem for linear systems under Gaussian noise has been presented by Kalman [1]. The Kalman filter provides the optimal state estimates in the minimum output prediction mean-square-error (MSE) sense for the given situation. The extensions of the idea to nonlinear systems and non-Gaussian noise scenarios include the standard extended Kalman filter (EKF) [2], analytical design efforts [3-5], and numerical approaches like the unscented Kalman filter (UKF) [6] and the particle filters (PF) [7].

The adaptive extended Luenberger observer (ELO) follows the mean-square-error optimality principle as in the Kalman filter framework, however, due to the difficulties in analytically updating the observer gains in a recursive manner in the nonlinear setup, the updates are performed using the stochastic gradient approach [8]. More detail on this observer scheme will be given in the following sections. At this point, it suffices to mention that for the linear system case, the relationship between the proposed adaptive observer and the Kalman filter becomes analogous to that of the least-mean-square (LMS) and recursive least squares (RLS) algorithms in adaptive filtering theory. The two algorithms, LMS and RLS, tackle the same problem using stochastic gradient updates and recursive optimal solution update, respectively. Both have their own advantages and disadvantages: Specifically, given noise-free input measurements, RLS tracks the optimal solution at every iteration, thus has much faster convergence properties. Nevertheless, while being relatively slower in convergence, LMS has added robustness properties when noisy input signals are available [8]. This property of LMS is not currently well understood in adaptive filtering theory, however, we would expect the ELO to demonstrate similar performance improvements under model uncertainty.[1]

In this paper, we will present two state-feedback control case studies using realistic models of internal combustion engines and induction machines. First, a brief overview of the ELO algorithm will be presented. Then, the closed-loop control of an internal combustion engine and an induction machine using state estimates obtained from ELO will be demonstrated.

2. Extended Luenberger Observer

Consider a general discrete-time, nonlinear and time-varying system of the form

[1] This paper will not focus on the investigation of robustness to model uncertainty issues of AELO. That study will be presented elsewhere.

$$\mathbf{x}_{k+1} = f(\mathbf{x}_k, \mathbf{u}_k, k)$$
$$\mathbf{y}_k = h(\mathbf{x}_k, \mathbf{u}_k, k) \quad (1)$$

where there are m inputs, n states, and l outputs. Although the system is nonlinear, we will still assume that a linear correction term will be sufficient to guarantee the asymptotic convergence of the state estimation error. Hence, the observer dynamics are

$$\tilde{\mathbf{x}}_{k+1} = f(\tilde{\mathbf{x}}_k, \mathbf{u}_k, k) + \mathbf{L}_k(\mathbf{y}_k - \tilde{\mathbf{y}}_k)$$
$$\tilde{\mathbf{y}}_k = h(\tilde{\mathbf{x}}_k, \mathbf{u}_k, k) \quad (2)$$

The i^{th} column of the observer gain matrix $\mathbf{L}_k$ is updated using the (approximate) stochastic gradient for output prediction error $\mathbf{e}_k = (\mathbf{y}_k - \tilde{\mathbf{y}}_k)$ according to [2]

$$\mathbf{L}^i_{k+1} = \mathbf{L}^i_k - \eta \frac{\partial(\mathbf{e}_k^T \mathbf{e}_k)}{\partial \mathbf{L}^i_k}$$
$$\frac{\partial(\mathbf{e}_k^T \mathbf{e}_k)}{\partial \mathbf{L}^i_k} = -2(\mathbf{y}_k - \tilde{\mathbf{y}}_k)^T h_x(\tilde{\mathbf{x}}_k, \mathbf{u}_k, k) \frac{\partial \tilde{\mathbf{x}}_k}{\partial \mathbf{L}^i_k} \quad (3)$$
$$\frac{\partial \tilde{\mathbf{x}}_k}{\partial \mathbf{L}^i_k} = \left[f_x(\tilde{\mathbf{x}}_{k-1}, \mathbf{u}_{k-1}, k-1) - \mathbf{L}^i_{k-1} \cdot h_x(\tilde{\mathbf{x}}_{k-1}, \mathbf{u}_{k-1}, k-1) \right] \frac{\partial \tilde{\mathbf{x}}_{k-1}}{\partial \mathbf{L}^i_{k-1}} + (\mathbf{y}^i_{k-1} - \tilde{\mathbf{y}}^i_{k-1}) \cdot \mathbf{1}_{nxn}$$

where $\mathbf{1}_{nxn}$ is an all-ones square matrix of size n [9]. In (3), f_x and h_x denote the Jacobians of the system equations with respect to the state vector.

3. Air-Fuel Ratio Control

In this section, we will demonstrate the performance of a closed-loop air-fuel ratio (AFR) control system for an internal combustion (IC) engine. This problem is of practical importance for the efficiency of the exhaust treatment system as manufacturers are mandated to observe strict regulations on exhaust emissions. In order to ensure the maximum conversion efficiency, it is required to keep the ratio of air mass and fuel mass in each cylinder at stoichiometry. Denoting the stoichimoetric AFR by AFR_s, the normalized AFR is

$$\lambda = \frac{m_a}{m_f} \frac{1}{AFR_s} \quad (4)$$

The goal of the AFR control problem is to keep λ as close as possible to unity. The difficulty arises from the fact that airflow dynamics are nonlinear and nonstationary. In addition, the event-based nature of the reciprocating engine introduces long time delays into the control problem. These delays limit the achievable closed-loop bandwidth by feedback, but this limitation can be circumvented by employing an observer to estimate the states of the plant.

[2] The actual gradient is slightly more complicated since it takes $\partial \mathbf{L}_k / \partial \mathbf{L}_{k-1}$ into account. However, for a small step size the additional terms are negligible.

In designing engine control systems, often mean value engine models are used. These models describe the mean engine state behavior over an engine cycle. These models can be constructed in time- or crank-angle domains; the transformation between these models is given by $\partial t = \partial \theta / 6N$, where θ is the crank-angle in degrees and N is the engine speed in rpm [10,11].

$$P_{m,k+1} = P_{m,k} + \frac{T_s}{V_m}\left(\frac{(\gamma-1)}{6N} h_t (T_w - T_{m,k}) + \gamma \cdot R(T_{amb}\dot{m}_{at,k} - T_{m,k}\dot{m}_{ac,k})\right)$$
$$T_{m,k+1} = T_{m,k} + \frac{T_s R T_m}{V_m P_m}\left(\frac{\gamma-1}{6NR} h_t (T_w - T_{m,k}) + (\gamma \cdot T_{amb} - T_{m,k})\dot{m}_{at,k} + (1-\gamma) T_m \dot{m}_{ac,k}\right) \quad (4)$$
$$m_{fp,k+1} = (1-\mu_p) m_{fp,k} + (1-\mu_i)\dot{m}_{fi,k}$$
$$\dot{m}_{fc,k} = \mu_p m_{fp,k} + \mu_i \dot{m}_{fi,k}$$
$$\lambda_{c1,k+1} = \lambda_{c,k} \quad \lambda_{c2,k+1} = \lambda_{c1,k}$$
$$\lambda_{c3,k+1} = \lambda_{c2,k} \quad \lambda_{c4,k+1} = \lambda_{c3,k}$$
$$\lambda_m(k+1) = \tau_m \lambda_m(k) + (1-\tau_m)\lambda_{c4}(k)$$
$$y_k = \lambda_{m,k}$$

2.1. Internal Combustion Engine Model

Assuming the time-domain approach, the discrete time mean-value model for an IC engine is given by (4). This model consists of 8 states, 2 inputs, and 1 output. The states are the manifold pressure (P_m), manifold temperature (T_m), wall-wetting mass (m_{fp}), time-delay associated with the transportation of the air-fuel charge within the cylinder and the exhaust system from the intake stroke to the AFR sensor. The inputs are throttle angle and injected fuel mass. The output is the measured AFR.

The amount of delay depends on the sampling rate in the discrete-time system. Taking an average delay of 500° for the mixture to reach the exhaust port following compression and power strokes, including an approximate 220° for transportation from the exhaust port to the AFR sensor, and assuming a sampling rate of 180°, we obtain 720/180=4 delay units.[3] In addition, a first-order linear dynamical AFR sensor with a time constant of τ_m is assumed.

The state equations for P_m and T_m are obtained from the conservation of energy. Here, V_m is the manifold volume, γ is the specific heat ratio for air, h_t is the heat transfer coefficient, T_w is the manifold wall temperature, R is the specific gas constant for air, T_{amb} is the ambient air temperature, $\dot{m}_{at}$ is the throttle air flow rate and $\dot{m}_{ac}$ is the

[3] All angles measured in degrees here are the crank-angle degrees.

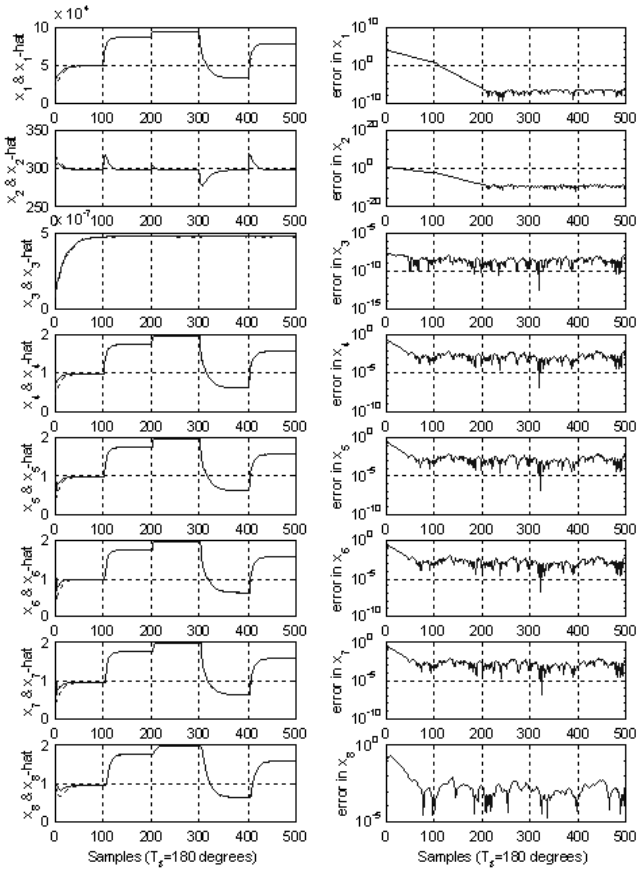

Figure 1. Actual and estimated state values for a sequence of step inputs (left). The state estimation errors (right).

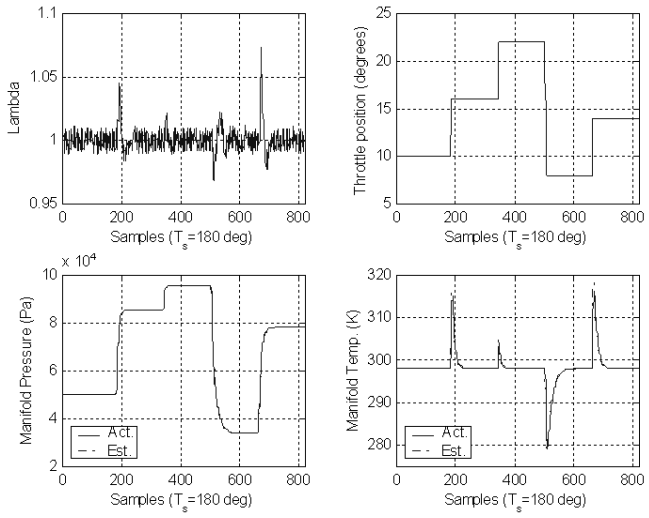

Figure 2. The normalized AFR (top-left), the control input (top-right), the manifold pressure (bottom-left), and the manifold temperature (bottom-right) in time.

air flow rate to the cylinder. The airflow rate is described by the standard orifice equation for compressible flow

$$\dot{m}_{at} = \frac{A_{th}(k)P_{amb}}{6N\sqrt{RT_{amb}}}\, g(P_m(k)) \tag{5}$$

where $g(.)$ is a nonlinear function and A_{th} is a nonlinear function of the throttle angle α [10,11]. The values of cylinder airflow rate can be obtained from steady-state engine mappings:

$$\dot{m}_{ac,k} = c_1 P_{m,k} + c_2 N_k + c_3 P_{m,k} N_k + c_4 P_{m,k}^2 + c_5 N_k^2 \tag{6}$$

The fuel dynamics must also be considered, since some of the fuel injected to the intake port does not enter the cylinders immediately and is deposited on the manifold wall in liquid form instead. This phenomenon is called the wall-wetting problem and can cause large deviations in normalized AFR if not properly compensated for. The fuel dynamics in (4) are derived based on a widely accepted wall-wetting model [12] and selecting proper parameter values depending on the operation regime [11], where $\dot{m}_{fi}$ is the mass flow rate of the injected fuel, $\dot{m}_{fc}$ is the mass flow rate of the fuel entering the cylinder. The parameters μ_p and μ_i are generally time-varying based on the evaporation time-constant of the fuel and the percentage of injected fuel hitting the wall.[4]

In order to demonstrate the estimation performance of ELO, we present in Fig. 1 a simulation result where various values of step inputs are given to the system and the AFR measurements are corrupted by white Gaussian noise. The estimation error for the states is bounded from below by the power of the measurement noise.

2.2. AFR Control Law

The desired amount of fuel mass in each cylinder is simply $m_{fc}(k) = m_{ac}(k) / AFR_s$. This can be achieved if the injected fuel mass is equal to

$$\dot{m}_{fi,k} = \frac{1}{\mu_i}\left(\frac{\dot{m}_{ac,k}}{AFR_s} - \mu_p \dot{m}_{fp,k}\right) \tag{7}$$

In practice, the controller will have access to estimates of m_{fp} offered by the observer.

In Fig. 2, we present an example simulation result where this control law is implemented using the state estimates given by ELO. In this case study, the observer utilizes the discrete-time model approximation provided in the previous section, while the actual system is simulated in continuous-time (using the Runge-Kutta4 integration technique). In this particular simulation, the worst-case deviation of the normalized AFR from unity is less than 7%. Such *spiky* deviations are observed to occur especially at the sudden transition points in the system input, which indicates that the cause of these unusual errors is the modeling inaccuracies of

[4] In this paper, we will assume that the engine speed is constant at 1500 rpm and that the fuel dynamics are time-invariant.

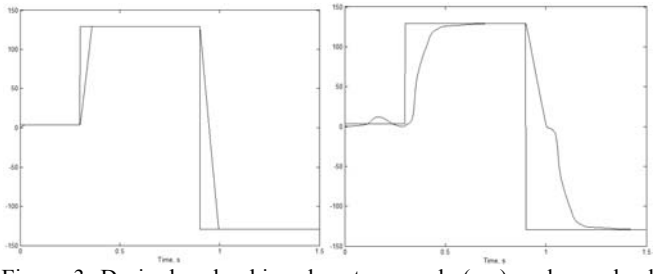

Figure 3. Desired and achieved motor speeds (rps) under no-load by the closed-loop control system using ELO estimates (left) and the reduced order observer estimates (right).

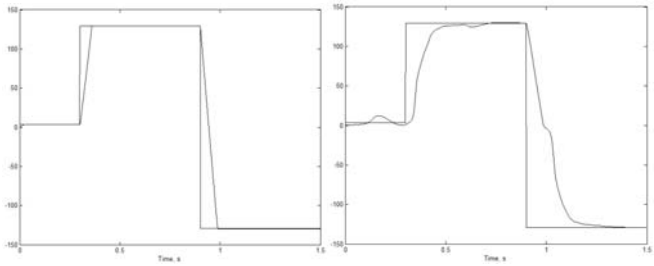

Figure 4. Desired and achieved motor speeds (rps) under 10% load by the closed-loop control system using ELO estimates (left) and the reduced order observer estimates (right).

the discretized equations in approximating the continuous-time dynamics. Hence, it is possible to reduce such errors by increasing the sampling time of the observer. This performance increase, nevertheless, will come at the cost of increased number of states in the model.

3. Induction Motor Control

Accurate rotor flux estimation is a key requirement in the success of direct vector control (DVC) of induction machines. Therefore, it has been the subject of continued research in power electronics and drives. Various approaches including estimation theory [13] and time-varying reduced-order observers [14] have been applied to solve this problem satisfactorily. In this section, we will demonstrate the performance of ELO in DVC of induction machines and compare it to that of the time-varying reduced-order observer under no-load and low torque conditions in the especially difficult situation of low driving voltage (75V dc link voltage) and low speeds.

In the stator frame of reference, the continuous-time model of an induction machine is given by [15]:

$$\begin{bmatrix} \dot{i}_{ds} \\ \dot{i}_{qs} \\ \dot{\varphi}_{dr} \\ \dot{\varphi}_{qr} \end{bmatrix} = \begin{bmatrix} A_x & 0 & A_y & A_\omega \omega_r \\ 0 & A_x & -A_\omega \omega_r & A_y \\ A_m & 0 & -T_r & -\omega_r \\ 0 & A_m & \omega_r & -T_r \end{bmatrix} \begin{bmatrix} i_{ds} \\ i_{qs} \\ \varphi_{dr} \\ \varphi_{qr} \end{bmatrix} + \begin{bmatrix} A_z & 0 \\ 0 & A_z \\ 0 & 0 \\ 0 & 0 \end{bmatrix} \begin{bmatrix} V_{ds} \\ V_{qs} \end{bmatrix} \quad (8)$$

$$\dot{\omega}_r = -T_m \omega_r + A_t \left(i_{qs} \varphi_{dr} - i_{ds} \varphi_{qr} \right) - A_s T_l$$

All coefficients A and T are constants determined by the machine geometry. The state vector consists of stator current and rotor flux components in the q and d axes, as well as the rotor speed. The input vector consists of the stator voltages along these axes. The output measurements of this plant include the two stator current components and the rotor speed. For use with ELO, these equations can be discretized using the forward difference approximation for the time derivative. The state vector estimate is used for feedback and the control inputs are generated using PI controllers [15].

In our simulation examples the dc link voltage is kept low (V_{dc} = 75V). The speed command is first set to 10% of the rated speed for 0.3s, then it is increased to 35% for 0.6s, and finally it is switched to 35% in the reverse direction for another 0.6s. The first case is under no load (Fig. 3) and the second case is under 10% of the rated load (Fig. 4) torque conditions for the same speed command and dc link voltage. For comparison, the closed-loop control system is operated using estimates from ELO as well as the reduced-order observer mentioned above. These simulation results (including the state vector tracking results and the electromagnetic torque response results not shown here for space considerations) demonstrate the superiority of ELO over the reduced order observer.

4. Conclusions

The adaptive extended Luenberger observer scheme is described in this paper. This observer uses the same optimality principles as the Kalman filter and the same stochastic gradient approach for the highly appreciated LMS algorithm in adaptive filtering theory. The use of a stochastic gradient approach allows a seamless extension of the Kalman filter principles to adaptive state estimation for nonlinear (and possibly time-varying) dynamical systems. In the current version of the adaptive ELO, the noise covariances are assumed to be identity. However, in the case of spatially colored noise vectors, the criterion and the associated update rule can be modified accordingly to yield asymptotically optimal performance.

We have demonstrated the power of this adaptive observer algorithm in two realistic closed-loop control problems: internal combustion engine air-to-fuel ratio control and direct vector control of induction machines. In both applications, the proposed observer performed satisfactorily without any need for initial parameter selections or fine-tuning of any coefficients. The only parameter to be selected is the stochastic gradient step size, which presents a trade-off between adaptability power and estimation accuracy.

Future work will demonstrate the necessary modifications and the performance under spatially colored and non-Gaussian noise scenarios. In addition, stability conditions and convergence dynamics of the adaptive nonlinear observer will be studied. There exists a broad literature

about designing nonlinear Luenberger observers under the gain scheduling framework. The stability conditions derived in this literature are expected to either readily apply to the adaptive ELO or be valid with minor modifications.

Acknowledgments

Parts of this work were done when A.U. Genc was at the University of Cambridge and was supported jointly by the UK EPSRC and Ford Motor Company. D. Erdogmus and J.C. Principe are supported by NSF grant ECS-0300340.

References

[1] R.E. Kalman, "A New Approach to Linear Filtering and Prediction Problems," *Trans. ASME - Journal of Basic Engineering*, vol. 82 (Series D), 1960, pp. 35-45.

[2] P.S. Maybeck, *Stochastic Models, Estimation, and Control*, Academic Press, NY, 1982.

[3] K.S. Narendra, K. Parthasarathy, "Identification and Control of Dynamical Systems Using Neural Networks," *IEEE Trans. Neural Networks*, vol. 1, 1990, pp. 252-262.

[4] M.M. Gupta, D.H. Rao (eds), *NeuroControl Systems: Theory and Applications*, IEEE Press, NY, 1994.

[5] W.T. Miller, R.S. Sutton, P.J. Werbos (eds), *Neural Networks for Contro*l, MIT Press, Cambridge, MA, 1995.

[6] S. Julier, J.K. Uhlmann, "A New Extension of the Kalman Filter to Nonlinear Systems," *Aerospace-Defense Sens. Simul. Controls*, Orlando, FL, 1997, pp. 182-193.

[7] A. Doucet, N. deFreitas, N. Gordon (eds), *Sequential Monte Carlo Methods in Practice*, Springer, NY, 2001.

[8] S. Haykin, *Adaptive Filter Theory*, 3rd ed., Prentice-Hall, NJ, 1996.

[9] D. Erdogmus, A.U. Genc, J.C. Principe, "A Neural Network Perspective to Extended Luenberger Observers," *Measurement & Control*, vol. 35, 2002, pp. 10-16.

[10] J.D. Powell, N.P. Fekete, C.F. Chang, "Observer-Based Air-Fuel Ratio Control," *IEEE Cont. Sys. Mag.*, vol. 18, no. 5, 1998, pp. 72-83.

[11] A. Chevalier, C.W. Vigild, E. Hendricks, "Predicting the Port Air Mass Flow of SI Engines in Air-Fuel Ratio Control Applications", *SAE 2000 World Congress*, 2000.

[12] C.F. Aquino, "Transient A/F Control Characteristics of the 5-Liter Central Fuel Injection Engine," *SAE*, 810494, 1981.

[13] G.C. Verghese, S.R. Sanders: "Observers for Flux Estimation in Induction Machines," *IEEE Trans. Industrial Electronics*, vol. 35, no. 1, 1988, pp. 85-94.

[14] A.K.Chattopadhya, N.K.De and A.N.Thakur: "Studies on A Rotor Flux Observer-based Direct Type Vector Controlled Induction Motor," Technical Report, Indian Institute of Technology, Kharagpur, India.

[15] R. Krishnan, *Electric Motor Drives Modeling, Analysis, and Control*, Prentice-Hall, New Jersey, 1996.